SCIREA Journal of Mechanics

http://www.scirea.org/journal/Mechanics

October 27, 2016

Volume 1, Issue1, October 2016

Prediction of Heat Transfer to Fully Developed Pipe Flows with a Modified Power Law Viscosity Model

Md. Mamun Molla[a], S. Ghosh Moulic[b] and Lun-Shin Yao[c,*]

[a]Department of Mathematics & Physics, North South University, Dhaka, Bangladesh.

E-mail: mamun.molla@northsouth.edu

[b]Department of Mechanical Engineering, Indian Institute of Technology, Kharagpur, Kharagpur 721302, India

E-mail: moulic@mech.iitkgp.ernet.in

[c,*]School for Engineering of Matter, Transport and Energy, Arizona State University, Arizona, 85287, USA.

E-mail: ls_yao@asu.edu

Abstract

Fully-developed forced convection heat transfer of a pseudoplastic fluid in a uniformly heated circular tube has been studied. The model used is a modification of the two-parameter Ostwald-de Waele power law, which correctly represents the upper and lower regions of Newtonian behavior shown by pseudoplastic or shear-thinning polymer melts and solutions. Results for a shear-thinning polymer solution, for which experimental data for the apparent viscosity is available over a large range of shear-rate magnitudes, predicted using the modified power-law

viscosity model, have been presented. A *new* non-dimensional shear-rate parameter governing the flow has been identified. The non-Newtonian fluid mechanics community has been unaware of the existence of this parameter. The paradox in the prediction of boundary layer flows caused by lack of knowledge of this parameter has been well documented by our previous studies. In this paper, we discuss it for non-boundary-layer flows. The momentum and energy equations have been solved numerically, for fully developed pipe flow, by the trapezoidal rule and finite volume method respectively. The results indicate that there are three regimes of flow. When the shear-rate parameter is small, the fluid behaves like a Newtonian fluid and the Nusselt number is identical to that for a Newtonian fluid. At intermediate values of the shear-rate parameter, there are two regions of flow: a central region where the fluid behaves like a Newtonian fluid and an outer region where the fluid behaves like a power-law fluid. The Nusselt numbers predicted by the modified power law and power law models agree in this intermediate range of shear rates. When the shear-rate parameter is large, there are two Newtonian regions, one near the axis and one near the wall, with a middle power-law zone.

Key words: Non-Newtonian fluid, modified power-law, forced convection heat transfer, Boger's experimental data

Nomenclature

A	non-dimensional shear-rate parameter
a	radius of pipe
C	Consistency of the power-law fluid
D	non-dimensional apparent viscosity
f_{MPL}	modified power-law function
f_{PL}	power-law function
$\mathbf{g}$	gravitational acceleration
L	length scale introduced by power law
n	non-Newtonian power-law index
Nu	Nusselt number
$\overline{P}$	Dimensional piezometric pressure

Pe	Peclet number
$\mathbf{r}$	position vector
r	non-dimensional radial coordinate
$\bar{r}$	dimensional radial coordinate
S	ratio of upper and lower threshold shear-rates
T	dimensional temperature
T_{w}	wall temperature
T_0	reference wall temperature
w	non-dimensional axial component of velocity
$\bar{w}$	dimensional axial component of velocity
w_{av}	non-dimensional average velocity
$(w_{av})_{MPL}$	non-dimensional average velocity predicted by modified power law
$(w_{av})_{PL}$	non-dimensional average velocity predicted by power law
$\bar{W}_0$	velocity scale
$\bar{z}$	dimensional axial coordinate
z	non-dimensional axial coordinate

Greek symbols

α	thermal diffusivity of the fluid
Γ	non-dimensional shear-rate magnitude normalized by lower threshold shear-rate
γ	non-dimensional shear-rate magnitude
$\bar{\gamma}$	dimensional shear-rate magnitude
$\bar{\gamma}_1$	dimensional lower threshold shear rate
$\bar{\gamma}_2$	dimensional upper threshold shear rate
μ	apparent viscosity of the non-Newtonian fluid
μ_0	zero-shear-rate viscosity
μ_∞	infinite-shear-rate viscosity
μ_{R}	ratio of infinite-shear-rate and zero-shear-rate viscosities
ρ	density of the fluid
τ	dimensional axial gradient of wall temperature
θ	non-dimensional temperature of the fluid

1. Introduction

The prediction of external flows of non-Newtonian fluids, using the power law model, has been the subject of extensive computations for more than fifty years. The limitations of the power law have been demonstrated in recent predictions of external flows, for forced, natural and mixed convection boundary layers [1-9]. This paper is concerned with internal forced convection of a non-Newtonian pseudoplastic fluid in a uniformly heated circular tube.

Non-Newtonian fluids may be broadly classified into three categories: viscous time-independent fluids, viscous time-dependent fluids and viscoelastic fluids. Comprehensive reviews of non-Newtonian fluid dynamics may be found in [10-14]. In this investigation, attention has been focused on purely viscous time-independent non-Newtonian fluids. The generalized Newtonian fluid model, obtained by replacing the viscosity of the Newtonian fluid by an apparent or non-Newtonian viscosity that depends on the magnitude of the rate-of-strain tensor, in Stokes law of viscosity and the Navier-Stokes equations, has been used in the analysis.

The simplest constitutive equation relating the apparent viscosity of a generalized Newtonian fluid to the shear rate is the two-parameter Ostwald-de Waele power law [10-14]. The shortcomings of the power law are well known. In the case of pseudo-plastic or shear-thinning fluids, the power law yields a physically unrealistic prediction of infinite apparent viscosity in the limiting case of zero shear rate and a zero apparent viscosity in the limit of infinite shear rate. The non-Newtonian viscosity of shear-thickening or dilatant fluids predicted by the power law model is zero in the limit of zero shear rate, and becomes unbounded in the limiting case of infinite shear rate. Infinite shear rates occur at the leading edge of forced convection and mixed convection boundary-layer flows. Zero shear rates occur near the outer edge of boundary-layer flows, at the leading edge of natural convection boundary-layer flows, and at the centerline of axisymmetric pipe flows. The Ostwald-de Waele power law model introduces non-physical singularities in boundary-layer formulations, at the leading edge and near the outer edge of the boundary-layer. Various matching techniques have been tried to remove those singularities, without success. These singularities are introduced due to the physically unrealistic prediction of zero and infinite viscosity by the power law model. Boger [15] pointed out, more than thirty years ago, that many non-Newtonian fluids behave like Newtonian fluids at very low and very high shear-rates, with constant apparent viscosities referred to as the zero-shear-rate viscosity and

the infinite-shear-rate viscosity; the power-law variation of the apparent viscosity occurs only in a certain intermediate range of values of the shear-rate magnitude. Unfortunately, this fundamentally important contribution is not well known in the Heat Transfer Community; the physically unrealistic power law is still a popular model.

Recently, a modified power-law viscosity model was proposed [1], in which the Ostwald-de Waele power law is used to determine the non-Newtonian viscosity for a certain range of the magnitude of the shear rate; outside this range of shear-rate magnitude, the viscosity was assumed to be independent of the shear rate. When the magnitude of the shear rate is lower than a certain threshold shear rate, referred to as the lower threshold shear rate, the viscosity is set equal to the zero-shear-rate viscosity. When the magnitude of the shear rate exceeds a certain threshold shear rate, referred to as the upper threshold shear rate, the viscosity is set equal to the infinite-shear-rate viscosity. This is consistent with the measurements of the apparent viscosity of a pseudoplastic fluid by Boger [15]. The modified power law does not predict zero or infinite values of the apparent viscosity in the limiting cases of zero and infinite shear rates. Thus, the singularities introduced in the boundary-layer equations by the popular Ostwald-de Waele power-law model do not appear when the modified power law is used [1-9].

In this investigation, the modified power law proposed in [1] has been used to study thermally developed flow in a uniformly heated circular tube, which is a typical example of internal forced convection. The study of forced convective heat transfer to non-Newtonian fluids in pipes is of fundamental importance, and has applications in chemical and process industries. The physics of non-Newtonian fluids has been clearly demonstrated without computing complex flow structures. The analysis shows that the usual non-dimensionalization used in the study of fully developed forced convection of a Newtonian fluid in a circular tube cannot be used to describe fully developed forced convection of a non-Newtonian fluid. An additional shear-rate parameter is required to fully characterize the flow of non-Newtonian pseudoplastic fluids. This non-dimensional shear-rate parameter, to our knowledge, has not been reported before.

In recent years, entropy-based design has become an emerging design methodology that uses the second law of thermodynamics along with the techniques of computational fluid dynamics to obtain optimized flow configurations in diverse industrial applications such as power generation, energy storage and aerodynamics. A comprehensive review of second law analysis in

thermodynamic optimization may be found in [16, 17]. It is worth noting that estimation of the local rates of entropy generation in engineering devices using non-Newtonian pseudoplastic fluids requires knowledge of the variation of the apparent viscosity of the non-Newtonian fluid with shear rate. Inaccuracies in the determination of the apparent viscosity may lead to erroneous non-optimal design. In particular, physically unrealistic predictions of infinite apparent viscosities of shear-thinning fluids by the power law model, in regions of zero shear rates, may introduce singularities in the function determining the local rates of entropy generation. The modified power law used in this study does not suffer from this drawback of the power law, and yields physically realistic predictions.

Results have been obtained for a shear-thinning polymer solution for which experimental data for the apparent viscosity is available over a wide range of shear rates [15]. The empirical parameters of the modified power law have been determined to fit the experimental data for the apparent viscosity reported by Boger [15], which, to our knowledge, is the only set of complete data available in the open literature. The fully developed velocity and temperature fields predicted by the modified power law model with the parameters fitting the rheological data of Boger [15] have been compared with those predicted using the power law model with the same power-law index. The results show the range of the shear-rate parameter in which the power law can be a good approximation.

2. Analysis

Steady laminar axisymmetric fully developed flow of a constant-density non-Newtonian fluid through a uniformly heated circular tube of radius 'a', driven by an externally applied pressure gradient, has been studied. It is convenient to use cylindrical coordinates $(\bar{r}, \bar{z})$ to describe the axisymmetric flow, where $\bar{z}$ is a coordinate along the axis of the pipe, and $\bar{r}$ is the radial coordinate measured from the axis. The swirl component of velocity is zero, and the axial component of velocity, $\overline{w}$, is a sole function of the radial coordinate $\bar{r}$. The no-penetration boundary condition at the surface of the pipe and the continuity equation imply that the radial component of velocity is zero in the fully developed region of the axisymmetric flow where the axial component of fluid velocity is axially invariant.

2.1 The governing equations

The generalized Newtonian fluid model has been used in this investigation. The equations describing balance of momentum are the Navier-Stokes equations with a shear-rate-dependent viscosity. The balance of momentum in the radial and azimuthal directions show that the piezometric pressure, $\overline{P} = \overline{p} - \rho\, \mathbf{g}\cdot\mathbf{r}$, is a sole function of $\overline{z}$. Here, $\overline{p}$ is the pressure, ρ is the fluid density, **g** is the gravitational acceleration and **r** is the position vector. The balance of momentum in the axial direction reduces to

$$\frac{1}{\overline{r}}\frac{d}{d\overline{r}}\left(\mu\,\overline{r}\,\frac{d\overline{w}}{d\overline{r}}\right) = \frac{d\overline{P}}{d\overline{z}}, \tag{1}$$

where μ is the non-Newtonian viscosity. The apparent viscosity, μ, of the generalized Newtonian fluid depends on the shear-rate magnitude,

$$\overline{\gamma} = \left|\frac{d\overline{w}}{d\overline{r}}\right|. \tag{2}$$

Thus, equation (1) is a nonlinear ordinary differential equation, unlike the momentum equation for a Newtonian fluid. The balance of energy is described by

$$\overline{w}\frac{\partial T}{\partial \overline{z}} = \alpha\left[\frac{1}{\overline{r}}\frac{\partial}{\partial \overline{r}}\left(\overline{r}\,\frac{\partial T}{\partial \overline{r}}\right) + \frac{\partial^2 T}{\partial \overline{z}^2}\right], \tag{3}$$

where $T(\overline{r},\overline{z})$ is the fluid temperature and α is the thermal diffusivity of the fluid.

Equations (1) and (3) involve three unknown functions, $\overline{w}(\overline{r})$, $T(\overline{r},\overline{z})$ and $\frac{d\overline{P}}{d\overline{z}}(\overline{z})$. A separation of variables argument shows that each side of equation (1) is a constant. Thus, the axial gradient of the piezometric pressure may be expressed as

$$\frac{d\overline{P}}{d\overline{z}} = -\overline{G}, \tag{4}$$

where $\overline{G}$ is a constant. When $\overline{G}$ is positive, the fluid flows in the positive $\overline{z}$ direction. If $\overline{G}$ is negative, the fluid flows in the negative $\overline{z}$ direction. The volume flow rate through the pipe depends on the value of the externally applied constant pressure gradient, $\overline{G}$.

In this investigation, the constitutive relation proposed by Yao and Molla [1], which is a modification of the power-law model, has been used to relate the apparent viscosity to the magnitude of the shear rate. The prediction of the modified power law has been compared with the prediction of the power law.

2.1.1. The Power-Law (PL) Viscosity Model

The shear-rate dependent viscosity for a power-law fluid is given by

$$\mu = f_{PL}\left(\bar{\gamma}; C, n\right) = C\,\bar{\gamma}^{n-1}. \qquad (5)$$

Equation (5) involves two parameters that characterize the fluid: a dimensional parameter, *C*, and a dimensionless parameter, *n*. The dimensions of the parameter, *C*, referred to as the fluid consistency, depends on the power-law index, *n*.

When $n > 1$, the fluid is said to be dilatant or shear-thickening. Equation (5) predicts that the apparent viscosity of shear-thickening fluids goes to zero as the shear rate approaches zero, and increases without bound as the shear rate is increased. The viscosity predicted by the power law model (5) is independent of the shear rate when $n = 1$. This corresponds to the special case of a Newtonian fluid. When $n < 1$, the fluid is said to be pseudoplastic or shear-thinning. Equation (5) indicates that the apparent viscosity of shear-thinning fluids is infinite in the limit of zero shear rate, and approaches zero as the shear rate is increased.

2.1.2 The Modified Power-Law (MPL) Viscosity Model

Experimental data indicates that many non-Newtonian fluids, such as polymeric fluids, exhibit Newtonian behavior at very low and very high shear rates, with constant apparent viscosities referred to as the zero-shear-rate viscosity and the infinite-shear-rate viscosity respectively [9-14]; the power-law variation of the viscosity, described by equation (5), occurs only in an intermediate range of shear rates. To remove the unrealistic prediction of zero and infinite viscosity, Yao and Molla [1] proposed a simple modification of the Ostwald-de Waele power law. The variation of the apparent viscosity with shear-rate magnitude in the modified power-law proposed by Yao and Molla [1] is described by the constitutive equation

$$\mu = f_{MPL}(\bar{\gamma}; C, n, \bar{\gamma}_1, \bar{\gamma}_2, \mu_0, \mu_\infty) = \begin{cases} \mu_0, & \bar{\gamma} \le \bar{\gamma}_1 \\ C\,\bar{\gamma}^{n-1}, & \bar{\gamma}_1 \le \bar{\gamma} \le \bar{\gamma}_2 \\ \mu_\infty, & \bar{\gamma} \ge \bar{\gamma}_2 \end{cases}, \qquad (6)$$

where $\bar{\gamma}_1$ and $\bar{\gamma}_2$ are two threshold shear rates, μ_0 is the zero-shear-rate viscosity and μ_∞ is the infinite-shear-rate viscosity. The power-law is used to determine the viscosity when the shear-rate magnitude falls in the range $\bar{\gamma}_1 \le \bar{\gamma} \le \bar{\gamma}_2$; the viscosity is independent of the shear rate when the magnitude of the shear rate is outside the range $\bar{\gamma}_1 \le \bar{\gamma} \le \bar{\gamma}_2$. The viscosity predicted by equation (6) is the zero-shear-rate viscosity, μ_0, when the magnitude of the shear rate is smaller than the lower threshold shear-rate, $\bar{\gamma}_1$. The viscosity is set equal to the infinite-shear-rate viscosity, μ_∞, when the magnitude of the shear rate exceeds the upper threshold shear-rate, $\bar{\gamma}_2$.

It is worth noting that if $\bar{\gamma}_1$ is set to zero and $\bar{\gamma}_2$ to infinity, the power law covers the entire range of shear-rates. Thus, the Ostwald de Waele power law may be viewed as a special case of equation (6) when $\bar{\gamma}_1$ = 0 and $\bar{\gamma}_2$ is infinite, that is,

$$f_{MPL}(\bar{\gamma}; C, n, 0, \infty, \mu_0, \mu_\infty) = f_{PL}\left(\bar{\gamma}; C, n\right). \qquad (7)$$

For this special case when $\bar{\gamma}_1$ = 0 and $\bar{\gamma}_2$ is infinite, the values of μ_0 and μ_∞ are not required for determining the non-Newtonian viscosity.

The function defined by equation (6) is assumed to be a continuous function of $\bar{\gamma}$. When $\bar{\gamma}_1$ is non-zero, continuity of the function defined by equation (6), at $\bar{\gamma} = \bar{\gamma}_1$, requires that

$$\mu_0 = C\bar{\gamma}_1^{n-1}. \qquad (8)$$

Equation (8) gives a relation between μ_0 and $\bar{\gamma}_1$ when $\bar{\gamma}_1$ is non-zero. When $\bar{\gamma}_2$ is finite, continuity of the function defined by equation (6), at $\bar{\gamma} = \bar{\gamma}_2$, requires that

$$\mu_\infty = C\bar{\gamma}_2^{n-1}. \qquad (9)$$

Equation (9) gives a relation between μ_∞ and $\bar{\gamma}_2$ when $\bar{\gamma}_2$ is finite.

The modified power-law correlation, given by equation (6), is characterized by six parameters: *C*, *n*, $\bar{\gamma}_1$, $\bar{\gamma}_2$, μ_0 and μ_∞. Since $\bar{\gamma}_1$ is related to μ_0, as indicated by equation (8), and $\bar{\gamma}_2$ is related to μ_∞, as indicated by equation (9), the modified power law proposed by Yao and Molla [1] involves four independent parameters characterizing the fluid.

2.2 The boundary conditions

The momentum equation (1) has to be solved subject to the no-slip boundary condition,

$$\bar{w}(a) = 0, \tag{10}$$

at the surface, $\bar{r} = a$, of the pipe, and the symmetry condition,

$$\frac{d\bar{w}}{d\bar{r}}(0) = 0, \tag{11}$$

at the axis, $\bar{r} = 0$, of the pipe. The rotationally symmetric temperature distribution must also satisfy the symmetry condition,

$$\frac{\partial T}{\partial \bar{r}}(0, \bar{z}) = 0, \tag{12}$$

at $\bar{r} = 0$. The symmetry conditions (11) and (12) may be viewed as regularity conditions at the singular point, $\bar{r} = 0$, of the differential equations (1) and (3).

In thermally developed axisymmetric forced-convection in a pipe with uniform surface heat flux, the wall temperature and the bulk mean temperature of the fluid increase with axial distance along the pipe at the same rate [18]. Thus,

$$\frac{dT_w}{d\bar{z}} = \frac{dT_m}{d\bar{z}} = \tau, \tag{13}$$

where T_w is the wall temperature and T_m is the bulk mean temperature of the fluid. The temperature distribution must satisfy Fourier's law of heat conduction,

$$k\frac{\partial T}{\partial \bar{r}}(a, \bar{z}) = q_w, \tag{14}$$

at $\bar{r} = a$, where q_w is the surface heat flux at the tube wall and *k* is the thermal conductivity of the fluid. Global balance of energy, using the relation (14), shows that

$$\tau = \frac{2q_w}{\rho c_p \bar{w}_{av} a}, \tag{15}$$

[18], where c_p is the specific heat capacity of the fluid at constant pressure and $\bar{w}_{av}$ is the average velocity through the duct. Global conservation of mass shows that the value of the average velocity, $\bar{w}_{av}$, is the same at all cross-sections of the pipe, for constant-density incompressible flows. Equation (15) indicates that the wall temperature gradient, τ, is constant for flow of a constant-property fluid through a uniformly heated tube with constant heat flux, q_w, at the tube surface. It follows from equation (13) that the wall temperature increases linearly with distance along the axis of the pipe as

$$T_w(\bar{z}) = T_0 + \tau \bar{z}, \tag{16}$$

where T_0 is a reference wall temperature. The relation (16) has been used as a boundary condition for solving the energy equation in several investigations of convective heat transfer in flows through uniformly heated ducts [19-28], in place of the equivalent Neumann boundary condition (14). In this investigation, the thermal boundary condition at the tube wall has been taken to be

$$T(a,\bar{z}) = T_w(\bar{z}) = T_0 + \tau \bar{z}, \tag{17}$$

at $\bar{r} = a$, following the approach used in [19-28].

2.3. Non-dimensionalization

To non-dimensionalize the governing equations, the following nondimensional variables are introduced:

$$\left.\begin{aligned}
&r = \frac{\bar{r}}{a}, \quad z = \frac{\bar{z}}{a} \ \left(coordinates\right),\\
&w = \frac{\bar{w}}{\bar{W}_0} \qquad \left(velocity\right),\\
&D = \frac{\mu}{\mu_0} \qquad \left(viscosity\right),\\
&\gamma = \bar{\gamma}\ \bar{t}_{conv} \quad \left(shear-rate\ magnitude\right),\\
&\theta = \frac{T_w - T}{\Delta T_s} \quad \left(temperature\right).
\end{aligned}\right\} \tag{18}$$

Here, $\bar{t}_{conv}$ is a convective time scale defined by

$$\bar{t}_{conv} = \frac{a}{\bar{W}_0}, \tag{19}$$

$\bar{W}_0$ is a reference velocity and ΔT_s is a characteristic temperature scale. Appropriate choices of the velocity and temperature scales are discussed later in this section.

2.3.1 The non-dimensional momentum equation

Using the non-dimensional variables defined in equation (18), the momentum equation (1) may be written in non-dimensional form as

$$\frac{1}{r}\frac{d}{dr}\left(D\, r \frac{dw}{dr} \right) = -\mathscr{G}, \tag{20}$$

where $\mathscr{G}$ is a non-dimensional pressure gradient parameter defined by

$$\mathscr{G} = \frac{\bar{G} a^2}{\mu_0 \bar{W}_0}. \tag{21}$$

The non-dimensional apparent viscosity, *D*, of the non-Newtonian fluid depends on the non-dimensional shear-rate magnitude, γ. This non-dimensional shear-rate magnitude, γ, scaled by the reciprocal of the time scale, $\bar{t}_{conv}$, may be determined from the velocity field using

$$\gamma = \left| \frac{dw}{dr} \right|. \tag{22}$$

The relation (22) follows from equations (2) and (18). Two models have been considered in this investigation: the power law model and the modified power law model.

2.3.2 The non-dimensional power law

The constitutive relation (5) for the power law model may be expressed in non-dimensional form as

$$D = \left(A\gamma \right)^{n-1}, \tag{23}$$

where *A* is a non-dimensional parameter defined by

$$A = \frac{\bar{W}_0}{a}\left(\frac{C}{\mu_0}\right)^{\frac{1}{n-1}}. \tag{24}$$

It may be noted that the quantity, $\left(\frac{C}{\mu_0}\right)^{\frac{1}{n-1}}$, in the definition of the parameter *A* has the units of time. Thus, the power law introduces a characteristic time scale, $\bar{t}_{PL}$, defined by

$$\bar{t}_{PL} = \left(\frac{C}{\mu_0}\right)^{\frac{1}{n-1}}, \tag{25}$$

and a corresponding length scale, *L*, defined by

$$L = \bar{W}_0\,\bar{t}_{PL} = \bar{W}_0\left(\frac{C}{\mu_0}\right)^{\frac{1}{n-1}}. \tag{26}$$

The non-dimensional parameter, *A*, may be expressed as the ratio of the length scale, *L*, introduced by the power law to the radius of the pipe:

$$A = \frac{L}{a}. \tag{27}$$

The parameter, *A*, may also be expressed as the ratio of the characteristic time scale, $\bar{t}_{PL}$, introduced by the power law to the convective time scale, $\bar{t}_{conv}$:

$$A = \frac{\bar{t}_{PL}}{\bar{t}_{conv}}. \tag{28}$$

Equation (23) shows that the non-dimensional viscosity, *D*, for the power law model depends on the power law index, *n*, and a non-dimensional shear-rate magnitude, Γ, defined by

$$\Gamma = A\,\gamma. \tag{29}$$

Using equation (28), the non-dimensional shear-rate magnitude, Γ, defined by equation (29), may be written as

$$\Gamma = \bar{\gamma}\,t_{PL}. \tag{30}$$

Thus, Γ is a non-dimensional shear-rate magnitude, scaled by the reciprocal of the characteristic time scale, $\bar{t}_{PL}$, introduced by the power law.

2.3.3 The non-dimensional modified power law

The modified power law (6) may be written in non-dimensional form, in terms of the non-dimensional shear-rate magnitude, Γ, as

$$D = \begin{cases} 1, & \Gamma \le \Gamma_1 \\ \Gamma^{n-1}, & \Gamma_1 \le \Gamma \le \Gamma_2, \\ \mu_R, & \Gamma \ge \Gamma_2 \end{cases} \tag{31}$$

where μ_R is the ratio of the infinite-shear-rate and the zero-shear-rate viscosities, defined by

$$\mu_R = \frac{\mu_\infty}{\mu_0}, \tag{32}$$

Γ_1 is the non-dimensional lower threshold shear-rate, defined by

$$\Gamma_1 = \bar{\gamma}_1 \bar{t}_{PL} = \bar{\gamma}_1 \left(\frac{C}{\mu_0} \right)^{\frac{1}{n-1}}, \tag{33}$$

and Γ_2 is the non-dimensional upper threshold shear-rate, defined by

$$\Gamma_2 = \bar{\gamma}_2 \bar{t}_{PL} = \bar{\gamma}_2 \left(\frac{C}{\mu_0} \right)^{\frac{1}{n-1}}. \tag{34}$$

Substitution of the relations (8) and (9) into equations (33) and (34) shows that

$$\Gamma_1 = 1, \tag{35}$$

and

$$\Gamma_2 = S, \tag{36}$$

where

$$S = \frac{\bar{\gamma}_2}{\bar{\gamma}_1}. \tag{37}$$

Using equations (8) and (9), the ratio of the upper and lower threshold shear-rates, *S*, may be expressed in terms of μ_R as

$$S = \left(\mu_R\right)^{\frac{1}{n-1}}. \tag{38}$$

It is worth noting that the characteristic time scale, $\bar{t}_{PL}$, introduced by the power law may be expressed as the reciprocal of the lower threshold shear rate:

$$\bar{t}_{PL} = \frac{1}{\bar{\gamma}_1}. \tag{39}$$

The relation (39) follows from equations (8) and (25). Using equation (39), the non-dimensional shear-rate magnitude, Γ, defined by equation (30), may be expressed as

$$\Gamma = \frac{\bar{\gamma}}{\bar{\gamma}_1}. \tag{40}$$

Thus, in the light of the parameters introduced by the modified power law, the shear-rate magnitude, Γ, used to determine the non-dimensional viscosity for the modified power law as well as the Ostwald de-Waele power law, may be interpreted as a normalized shear-rate magnitude, scaled by the lower threshold shear rate. It may be noted that the parameter *A* may be written as

$$A = (\bar{W}_0 / a) / \bar{\gamma}_1, \tag{41}$$

using equations (19), (28) and (39). Since $(\bar{W}_0 / a)$ is a measure of the magnitude, $\left|\frac{d\bar{w}}{d\bar{r}}\right|$, of the shear rate, the parameter *A* may be interpreted as a non-dimensional shear-rate parameter.

2.3.4 The non-dimensional energy equation

In thermally developed flows through uniformly heated ducts, the wall temperature *relative* to the tube wall is independent of the axial coordinate [19-28]. Thus, the non-dimensional temperature, θ, defined in equation (18), is a sole function of the radial coordinate. It follows that that the axial gradient of the fluid temperature is a constant in thermally developed flows in uniformly heated tubes, given by

$$\frac{\partial T}{\partial \bar{z}} = \tau \,. \tag{42}$$

Equation (42) is an identity that holds at all points in the thermally developed region of the flow, and hence, can be differentiated partially with respect to $\bar{z}$. This yields the relation,

$$\frac{\partial^2 T}{\partial \bar{z}^2} = 0 \,. \tag{43}$$

Equation (43) shows that the axial conduction term in equation (3) is identically zero for thermally developed flows in uniformly heated tubes. This is a consequence of the fact that the wall temperature, T_w, is a linear function of $\bar{z}$ and the fact that θ is independent of *z*.

Using the non-dimensional variables defined in equation (18), the energy equation (3) may be expressed in non-dimensional form as

$$\frac{1}{r}\frac{d}{dr}\left(r\frac{d\theta}{dr} \right) + H\ w = 0. \tag{44}$$

Here, *H* is a non-dimensional temperature gradient parameter defined by

$$H = \frac{\tau a Pe}{\Delta T_s}, \tag{45}$$

and *Pe* is the Peclet number, defined by

$$Pe = \frac{\bar{W}_0\, a}{\alpha}. \tag{46}$$

It is worth emphasizing that the partial differential equation (3) representing local balance of thermal energy has reduced to the ordinary differential equation (44) in the thermally developed region of the flow, as the axial gradient of the fluid temperature is a constant and the axial conduction term is identically zero in thermally developed flows in uniformly heated tubes. The axial convection term in equation (3), which is independent of the unknown temperature field in the thermally developed region of the flow, appears in equation (44) as a space-dependent source term given by $H\ w(r)$.

2.3.5 The velocity scale

In this investigation, the reference velocity, $\bar{W}_0$, used to non-dimensionalize the fluid velocity, has been taken to be

$$\bar{W}_0 = \frac{\bar{G}a^2}{4\mu_0}. \tag{47}$$

This choice of velocity scale, obtained by balancing the orders of magnitude of the viscous term and the pressure gradient term in the momentum equation, makes the non-dimensional pressure gradient parameter, $\mathscr{G}$, on the right hand side of equation (20) constant, with a value of 4. Velocity scales based on the constant applied pressure gradient have been used in previous analyses of fully developed duct flows [20-23]. The factor of 4 in the definition of the velocity scale, $\bar{W}_0$, has been introduced so that the reference velocity defined by equation (47) represents the maximum or centerline velocity for the special case of Hagen-Poiseuille flow of a Newtonian fluid with viscosity equal to the zero-shear-rate viscosity, μ_0. This provides a rational basis for comparing the flow and heat transfer characteristics of non-Newtonian fluids with those of a constant-property Newtonian fluid with viscosity equal to the zero-shear-rate viscosity, μ_0. Since the shear rate is zero at the centerline of the pipe, as indicated by equation (11), the apparent viscosity of the non-Newtonian fluid at the centerline, predicted by the modified power law (6), is the zero-shear-rate viscosity, μ_0. Thus, it is appropriate to take the reference viscosity in the definition (47) of the velocity scale, $\bar{W}_0$, to be the viscosity of the non-Newtonian fluid at the centerline, namely, the zero-shear-rate viscosity.

2.3.6 The temperature scale

Following the approach of [20-28], the temperature scale, ΔT_s, used in the definition of the non-dimensional temperature has been taken to be

$$\Delta T_s = \tau aPe. \tag{48}$$

This choice of temperature scale, obtained by balancing the orders of magnitude of the radial conduction and the axial convection terms in the energy equation, makes the non-dimensional temperature gradient parameter, *H*, multiplying the convection term on the right hand side of the

non-dimensional energy equation (44) constant, with a value of 1. Thus, the non-dimensional energy equation becomes free of non-dimensional parameters.

2.3.7 The non-dimensional problem statement

Using the reference velocity, $\bar{W}_0$, defined by equation (47), the momentum equation (20) may be written as

$$\frac{d}{dr}\left(D r \frac{dw}{dr} \right) = -4 r, \tag{49}$$

The associated boundary condition (10) may be expressed in non-dimensional form as

$$w(1) = 0, \tag{50}$$

at $r = 1$. The non-dimensional velocity distribution must satisfy the regularity conditions,

$$\frac{dw}{dr}(0) = 0, \tag{51}$$

for axisymmetric flows, at the singular point, $r = 0$, of the cylindrical coordinate system.

Using the temperature scale, ΔT_s, defined by equation (48), the energy equation (44) may be written as

$$\frac{1}{r}\frac{d}{dr}\left(r \frac{d\theta}{dr} \right) + w = 0. \tag{52}$$

Equation (52) has to be solved subject to the boundary condition,

$$\theta(1) = 0, \tag{53}$$

at the surface, $r = 1$, of the pipe. The boundary condition (53) follows from equations (17) and (18). Rotational symmetry requires that the temperature distribution satisfy the regularity condition,

$$\frac{d\theta}{dr}(0) = 0, \tag{54}$$

at the axis, $r = 0$, of the pipe.

To complete the problem formulation, one needs to specify the constitutive equations relating the non-dimensional viscosity, D , to the non-dimensional shear-rate magnitude. The non-dimensional constitutive relation (23) for the power law model may be expressed in terms of the function f_{PL} , defined by equation (5), as

$$D = f_{PL}\left(\Gamma;1,n\right) = f_{PL}\left(A\gamma;1,n\right), \tag{55a}$$

where

$$f_{PL}\left(\Gamma;1,n\right) = \Gamma^{n-1}. \tag{55b}$$

Using the function f_{MPL} defined by equation (6), the non-dimensional constitutive relation (31) for the modified power-law viscosity model may be written in the form,

$$D = f_{MPL}(\Gamma;1,n,1,S,1,\mu_R) = f_{MPL}(A\gamma;1,n,1,S,1,\mu_R), \tag{56a}$$

where

$$f_{MPL}(\Gamma;1,n,1,S,1,\mu_R) = \begin{cases} 1, & \Gamma \le 1 \\ \Gamma^{n-1}, & 1 \le \Gamma \le S, \\ \mu_R, & \Gamma \ge S. \end{cases} \tag{56b}$$

The ratio of the upper and lower threshold shear rates, S , may be determined from the values of n and μ_R using equation (38). The non-dimensional shear-rate magnitude, Γ , used in equations (55) and (56), may be determined from the velocity field using the relation

$$\Gamma = A\left|\frac{dw}{dr}\right|. \tag{57}$$

The relation (57) follows from equations (22) and (29). Using the reference velocity, $\bar{W}_0$, defined by equation (47), the non-dimensional parameter, A, defined by equation (24), may be expressed as

$$A = \frac{\bar{G}\,a}{4\mu_0}\left(\frac{C}{\mu_0}\right)^{\frac{1}{n-1}}. \tag{58}$$

It is worth noting that for the special case of a constant-viscosity Newtonian fluid, μ_R =1 and n = 1. It follows from equation (38) that S = 1 for this special case. The constitutive relation (56) for the modified power law, with μ_R = 1, n = 1 and S = 1, reduces to

$$D = 1. \tag{59}$$

The constitutive relation (55) for a power law fluid also reduces to equation (59) for the special case of a Newtonian fluid (n = 1). The reference viscosity, μ_0, used in the definition of the non-dimensional viscosity given in equation (18), for the special case of a Newtonian fluid, should be interpreted as the constant viscosity of the fluid.

The velocity field is determined by solving the momentum equation (49), subject to the boundary conditions (50) and (51), with the non-dimensional viscosity, D, given by equation (55) or (56) or (59) and the shear-rate magnitude, Γ, obtained using equation (57). The velocity field predicted by the power law is determined using the constitutive equation (55). The prediction of the modified power law is obtained using the constitutive equation (56). For the special case of a Newtonian fluid, the constitutive equation (59) is used. Once the velocity field has been determined, the temperature field is obtained by solving the energy equation (52), subject to the boundary conditions (53) and (54).

The momentum equation (49) and the energy equation (52) are free of non-dimensional parameters. The associated boundary conditions are also free of non-dimensional parameters. Thus, the non-dimensional parameters describing the solution are the parameters in the constitutive equations relating the non-dimensional viscosity to the shear-rate magnitude, $\left|\frac{dw}{dr}\right|$.

2.3.8 The solution for a power-law fluid

Examination of equations (55) and (57) reveals that the constitutive equation for the power law involves the power law index, n, and the parameter, A, defined by equation (58). Thus, the solution predicted by the power law may be expressed in the functional form,

$$\left.\begin{aligned} w &= w_{PL}\left(r;n,A\right), \\ \theta &= \theta_{PL}\left(r;n,A\right), \end{aligned}\right\} \tag{60}$$

where the semicolons separate the non-dimensional parameters from the independent variable. The solution of the momentum equation for the power-law fluid is given in standard textbooks, e.g. [11]. The function, $w_{PL}(r;n,A)$, is given by

$$w_{PL}(r;n,A)=\frac{n}{n+1}\left(\frac{2}{A^{n-1}}\right)^{\frac{1}{n}}(1-r^{\frac{n+1}{n}}), \tag{61}$$

[29]. The function, $\theta_{PL}(r;n,A)$, is given by

$$\theta_{PL}(r;n,A)=\frac{n}{n+1}\left(\frac{2}{A^{n-1}}\right)^{\frac{1}{n}}\left[\frac{1}{4}\left(1-r^2\right)-\frac{n^2}{\left(3n+1\right)^2}\left(1-r^{\frac{3n+1}{n}}\right)\right]. \tag{62}$$

2.3.9 The solution for a Newtonian fluid

The solution for a Newtonian fluid, obtained by setting n = 1 in equations (61) and (62), may be expressed as

$$\left.\begin{aligned} w&=w_{Newt}\left(r\right),\\ \theta&=\theta_{Newt}\left(r\right),\end{aligned}\right\} \tag{63}$$

where $w_{Newt}\left(r\right)$ and $\theta_{Newt}\left(r\right)$ are universal functions independent of n and A. These universal functions are given by

$$w_{Newt}\left(r\right)=1-r^2, \tag{64}$$

$$\theta_{Newt}(r)=\frac{1}{16}\left(3-4r^2+r^4\right). \tag{65}$$

Equation (64) is the Hagen-Poiseuille velocity distribution for flow of a Newtonian fluid through a circular pipe. The solution (65) represents the non-dimensional temperature distribution in thermally developed flow of a Newtonian fluid through a uniformly heated circular tube [21].

2.3.10 The prediction of the modified power law

Equations (56) and (57) show that the constitutive equation for the modified power law involve the power law index, n, the ratio of zero-shear-rate and infinite-shear-rate viscosities, μ_R, the ratio of the upper and lower threshold shear rates, S, and the parameter, A, defined by equation

(58). The parameters n, μ_R and S are properties of the non-Newtonian fluid. The parameter, A, defined by equation (58), on the other hand, is a non-dimensional flow parameter, whose value depends on the externally applied pressure gradient, G. The non-dimensional velocity and temperature fields predicted by modified power law depend on the three fluid properties, n, μ_R and S, as well as the flow parameter A.

Equation (38) shows that the three fluid properties, n, μ_R and S, are related. Hence, only two of these three fluid properties are independent. It is convenient to take n and μ_R as the independent rheological properties of the fluid; the value of S can be calculated from the values of n and μ_R using equation (38). The solution predicted by the modified power law may thus be expressed by the functional form,

$$\left.\begin{aligned} w &= w_{MPL}\left(r; n, \mu_R, A\right), \\ \theta &= \theta_{MPL}\left(r; n, \mu_R, A\right). \end{aligned}\right\} \qquad (66)$$

Equations (60) and (66) show that the solution predicted by the modified power law and the power law depend on the non-dimensional flow parameter, A, unlike the solution (63) for a Newtonian fluid. Thus, the usual non-dimensionalization used in the study of fully-developed forced convection of a Newtonian fluid in a circular tube cannot describe the flow of a non-Newtonian fluid. An additional parameter, A, is required to fully characterize the flow of non-Newtonian pseudoplastic fluids.

2.3.11 Integral of the momentum equation.

Integration of the momentum equation (49) and application of the zero shear rate condition (51) at the axis of the pipe leads to the following relation:

$$D\frac{dw}{dr} = -2r\,. \qquad (67)$$

Equation (67) shows that the product of the non-dimensional viscosity and shear-rate magnitude, $D\left|\frac{dw}{dr}\right|$, increases monotonically with r from a zero value at the axis (r = 0) to a maximum value of 2 at the pipe wall (r = 1). This relation is valid for the modified power law model as well as the power law model. The relation (67) also holds for the special case of a

Newtonian fluid. Equation (67) forms the basis of the numerical method used to determine the solution of the momentum equation.

3. Numerical Method

The velocity and temperature distributions for the modified power law viscosity model have been determined by a numerical method. The method used to solve the momentum equation is described in section 3.1 The solution of the energy equation is discussed in section 3.2.

3.1 The solution of the momentum equation

Equation (67) was integrated numerically using the trapezoidal rule, after dividing by *D*. This leads to

$$w_j = w_{j+1} + \left(\left[\frac{r}{D} \right]_{j+1} + \left[\frac{r}{D} \right]_j \right) \Delta r \,, \tag{68}$$

where w_j is the approximate value of $w(r_j)$,

$$r_j = (j-1)\Delta r,\ j = 1, 2, ..., N \,, \tag{69}$$

$$\Delta r = \frac{1}{N-1} \,, \tag{70}$$

and *N* is the number of grid points. The no-slip boundary condition (50) implies that

$$w_N = 0 \,. \tag{71}$$

Equation (68) was solved iteratively with *D* calculated using equation (56), sequentially for $j = N-1, N-2, \ldots, 1$. The discrete boundary condition (71) was enforced in equation (68) for $j = N-1$. The iterations were continued until the difference between successive iterates was less than a tolerance, which has taken to be 10^{-6}. The value of Δr was taken to be 0.001.

3.2 The solution of the energy equation

The finite volume method has been applied to the energy equation (52) to get the solution for the temperature, $\theta(r)$. This leads to the following equation:

$$\frac{(r_S + r_P)}{(r_P - r_S)}\theta_S - \left[\frac{(r_S + r_P)}{(r_P - r_S)} + \frac{(r_N + r_P)}{(r_N - r_P)}\right]\theta_p + \frac{(r_N + r_P)}{(r_N - r_P)}\theta_N = -2\,rw\big|_P \Delta r \tag{72}$$

where *P* is the central node, *N* and *S* are the neighbouring nodes, *n* and *s* are cell faces, as shown in Figure 1. The discretised equation (72) can be written in tri-diagonal matrix form as

$$A_S\theta_S + B_P\theta_P + C_N\theta_N = S_c \tag{73}$$

where

$$A_S = \frac{(r_S + r_P)}{(r_P - r_S)},\ B_P = -\left[\frac{(r_S + r_P)}{(r_P - r_S)} + \frac{(r_N + r_P)}{(r_N - r_P)}\right],$$

$$C_N = \frac{(r_N + r_P)}{(r_N - r_P)},\ \text{and}\ S_c = -2rw\big|_P \Delta r \tag{74}$$

The algebraic equations (73) have been solved subject to boundary conditions (53) and (54), using the tridiagonal matrix algorithm [30].

4. Results and discussion

Results have been presented for the case of a shear-thinning polymer solution for which data for the variation of the apparent viscosity, measured over a large range of shear-rates, has been reported by Boger [15]. The independent rheological parameters, μ_R and *n*, of the modified power law have been determined to fit the data for the apparent viscosity in [15]. The variation of the apparent viscosity with shear-rate magnitude, predicted by the modified power law with these values of μ_R and *n*, is shown in Figure 2 in non-dimensional form. The rheological data reported in [15] has been shown in the figure, for comparison. Results for the velocity and temperature distribution in fully developed forced convection in a uniformly heated circular tube have been obtained, for several values of the non-dimensional flow parameter, *A*, using the modified power law model with the values of μ_R and *n* determined to fit the rheological data of Boger [15].

The radial distribution of the non-Newtonian viscosity, obtained by solving the momentum equation, is shown in Fig. 3 for six representative values of *A*. The variation of the non-dimensional wall shear-rate magnitude with the pressure-gradient dependent shear-rate parameter, *A*, is presented in Fig. 4, to elucidate the physics of the flow. The radial distributions of the axial velocity and temperature are shown in Figs. 5 and 6 respectively, for *A* = 0.05, 0.5, 1, 5, 50 and 750. The variation of the Nusselt number with the shear-rate parameter *A* is shown in Fig. 7. The predictions of the power law model for the same value of *n* are also shown in these figures, for comparison with the results obtained using the modified power law model. The solid lines in these figures indicate the prediction using the modified power law, while the dashed lines indicate the prediction of the power law.

4.1 The modified power law fit

The values of the zero-shear-rate and the infinite-shear-rate viscosites of the 0.4 % polyacrylamide solution used in the experiments of Boger [15] are 1.42 Pa s and 4 x 10^{-3} Pa s respectively. Thus,

$$\mu_0 = 1.42 \text{ Pa s}, \tag{75a}$$

$$\mu_\infty = 4 \text{ x } 10^{-3} \text{ Pa s}, \tag{75b}$$

and

$$\mu_R = 2.82 \text{ x } 10^{-3}, \tag{75c}$$

for this polyacrylamide solution. Data for the variation of the apparent viscosity with the shear rate, taken from reference [15], has been indicated in Figure 2 which shows the variation of the non-dimensional viscosity, *D*, with the non-dimensional shear-rate magnitude, Γ. The variation of *D* with Γ, predicted by the non-dimensional modified power law function defined by equation (56), is also plotted in Figure 2, for μ_R = 2.82 x 10^{-3} and *n* = 0.5242. A glance at Figure 2 reveals that the modified power law with *n* = 0.5242 and μ_R = 2.82 x 10^{-3}, is an excellent fit to the experimental data points indicated by the circles.

In the following sections, results obtained using the modified power law model with the following values of the parameters are presented:

$$n = 0.5242, \tag{76a}$$

μ_R = 2.82 x 10^{-3}, (76b)

S = 2.29 x 10^5. (76c)

The value of S shown in equation (76c) has been calculated using equation (38), with the values of n and μ_R given by equations (76a) and (76b). The prediction of the power law model has also been presented, for the value of n given in equation (76a).

4.2 Radial distribution of the non-Newtonian viscosity

The radial distributions of the non-dimensional shear-rate dependent viscosity, obtained by solving the momentum equation using the modified power law model, are plotted in Figures 3(a)-(f) for selected values of the shear-rate parameter A. The viscosity distributions predicted by the power law model with the same power-law index are also shown in these figures. The predictions of the modified power law model are shown by the solid lines; the dashed lines indicate the predictions of the power-law model.

The radial distribution of the non-dimensional non-Newtonian viscosity predicted by the power law model is given by

$$D = (2Ar)^{\frac{n-1}{n}}. \qquad (77)$$

The relation (77) follows from equations (55) and (67). Since $n < 1$, equation (77) predicts that $D \to \infty$ as $r \to 0$.

Using equations (56) and (67), the radial distribution of the non-dimensional non-Newtonian viscosity predicted by the modified power law model may be expressed as

$$D = \begin{cases} 1, \gamma \le \dfrac{1}{A} \\ (2Ar)^{\frac{n-1}{n}}, \dfrac{1}{A} \le \gamma \le \dfrac{S}{A}. \\ \mu_R, \gamma \ge \dfrac{S}{A} \end{cases} \qquad (78)$$

The expression (78) shows that the value of D at a given radial location depends on the local value of the shear-rate magnitude γ. Equations (77) and (78) show that when γ lies in the

range $\frac{1}{A} \le \gamma \le \frac{S}{A}$, the value of D predicted by the modified power law model at a given radial location is identical to that predicted by the power law model with the same power-law index.

Figure 3(a) shows that the non-dimensional viscosity predicted by the modified power law model is $D = 1$ at all points in the flow field, when $A = 0.05$. This may be explained by the fact that for very small values of A, the maximum shear-rate magnitude is less than the lower threshold shear-rate everywhere in the flow field. Thus, non-Newtonian behavior is not induced, and the fluid behaves like a Newtonian fluid with viscosity equal to the value of the zero-shear-rate viscosity. Figure 3(a) shows that the viscosity predicted by the power law model is everywhere higher than the constant viscosity, $D = 1$, predicted by the modified power law model. In particular, the power law model yields a physically unrealistic prediction of infinite apparent viscosity as $r \to 0$.

Figure 3(b) indicates that when $A = 0.5$, the non-Newtonian viscosity predicted by the modified power law model is $D = 1$ in the core region near the pipe axis, where the shear-rate magnitude is less than the lower threshold shear rate. A glance at Fig. 3(b) reveals that power-law behavior is predicted by the modified power law model in the outer region of the pipe where the shear-rate magnitude is larger than the lower threshold shear rate but smaller than the upper threshold shear rate. Thus, the fluid behaves like a Newtonian fluid with viscosity equal to the value of the zero-shear-rate viscosity in the central region of the pipe, and like a power-law fluid in the outer region of the pipe adjacent to the pipe wall. The viscosity predicted using the power law model agrees with the viscosity predicted by the modified power law model in the outer region of the region where γ lies in the range $\frac{1}{A} \le \gamma \le \frac{S}{A}$. Thus, as indicated by equations (77) and (78), the non-Newtonian viscosity predicted by the two models are identical in this region. The viscosity predictions of the two models differ in the central region of the pipe. The non-Newtonian viscosity predicted by the power law model is higher than the zero-shear-rate viscosity in the central region, and goes to infinity as $r \to 0$, as in the case when $A = 0.05$. It is worth emphasizing that predictions of apparent viscosities larger than the zero-shear-rate viscosity are physically unrealistic.

Figure 3(c) shows that the predictions of the modified power law model and the power law model for $A = 1$ are qualitatively similar to the predictions for $A = 0.05$. Comparison of Fig. 3(b) and Fig. 3(c) reveals that the size of the central Newtonian region near the axis where $D = 1$ is smaller

when A = 1. The size of the outer power-law region adjacent to the pipe wall is larger for A = 1. Figure 3(d) indicates that when A is increased to 5, the size of the central Newtonian region is so small that it is not visible on the scale of the graph. A key difference between the apparent viscosities predicted by the two models, however, is that D = 1 at r = 0 in the case of the prediction of the modified power law model, while D is infinite in the case of the prediction of the power law model.

Figure 3(e) shows the emergence of a second Newtonian region in the result predicted by the modified power law model, with constant non-dimensional viscosity $D = \mu_R$, in the layer adjacent to the pipe wall, when A = 50. In this region adjacent to the pipe wall, the power law model yields a physically unrealistic prediction of apparent viscosities lower than the infinite-shear-rate viscosity. The small Newtonian region near the axis of the pipe with constant non-dimensional viscosity D = 1, is not visible on the scale of the graph. The modified power law model predicts a power-law region between the Newtonian region near the axis and the Newtonian region adjacent to the pipe wall; in this middle region of the pipe, the apparent viscosity predicted by the modified power law model agrees with the apparent viscosity predicted using the power law model.

Figure 3(f) shows that the predictions of the modified power law model and the power law model for A = 750 are qualitatively similar to the predictions for A = 50. Comparison of Fig. 3(e) and Fig. 3(f) indicates that the size of the outer Newtonian region adjacent to the pipe wall, where $D = \mu_R$, is larger when A = 750. For both A = 50 and A = 750, the power law model yields physically unrealistic predictions of apparent viscosities lower than the infinite-shear-rate viscosity in the layer adjacent to the wall and infinite apparent viscosity at the axis.

Figs 3(a)-(f) show the existence of three regimes of flows characterized by the value of the shear-rate parameter A. These regimes may be classified as

(a) the low shear rate regime,

(b) the intermediate shear rate regime,

(c) the high shear rate regime.

The non-Newtonian fluid exhibits Newtonian behavior in the *low shear rate regime*. The *intermediate shear rate regime* is characterized by two regions of flow: an inner central region

near the axis where the non-Newtonian fluid exhibits Newtonian behavior, and an outer region adjacent to the pipe wall where the fluid behaves like a power-law fluid. In *the high shear rate regime*, there are three regions of flow: two distinct regions where the non-Newtonian fluid exhibits Newtonian behavior, one near the axis of the pipe where the non-dimensional apparent viscosity is D = 1 and one adjacent to the pipe wall where $D = \mu_R$, with a third middle region sandwiched between these two distinct Newtonian regions where the fluid behaves like a power-law fluid.

4.3 Variation of the non-dimensional wall shear-rate magnitude with *A*

The three regimes of flow are clearly visible in Fig. 4 which displays the variation of the non-dimensional wall shear-rate magnitude with the shear rate parameter *A*. The non-dimensional wall shear-rate magnitude, γ_w, is given by

$$\gamma_w = \left|\frac{dw}{dr}\right|_{r=1} = \frac{2}{D_w}, \qquad (79)$$

where D_w is the non-dimensional apparent viscosity at the wall. The relation (79) follows from equation (67).

Fig. 4 shows that the non-dimensional wall shear-rate magnitude, γ_w, predicted by the modified power law model is a constant, equal to 2, when *A* is small. This may be explained as follows. In this *low shear rate regime*, the fluid behaves like a Newtonian fluid with non-dimensional viscosity D = 1. Thus, the value of the non-dimensional wall viscosity is D_w = 1 for the modified power law model, when *A* is small. Equation (79) shows that the value of γ_w is 2 when D_w = 1. Fig. 4 indicates that the power law model under-predicts the value of the wall shear-rate magnitude in the low shear rate regime.

A glance at Fig. 4 reveals that the non-dimensional wall shear-rate magnitude, γ_w, predicted by the modified power law model is a constant at low values of the shear rate parameter *A*. As the shear rate parameter is increased beyond a certain threshold value, γ_w starts to increase linearly with *A* on the logarithmic scale of the graph. The wall shear-rate magnitude then saturates to a constant value when the shear-rate parameter exceeds another threshold value. In the intermediate shear rate regime, the non-dimensional wall viscosities predicted by the modified power law

model and the power law model are identical, and vary with A as $D_w = (2A)^{\frac{n-1}{n}}$. This may be inferred by referring to equations (77) and (78). It follows from equation (79) that in the intermediate shear rate regime, the non-dimensional wall shear-rate magnitude varies with A as $\gamma_w = \left(2A^{1-n}\right)^{\frac{1}{n}}$, for both the models. Consequently, the variation of γ_w with A is linear on a log-log plot, in this flow regime, for both the models.

When A is very large, the non-Newtonian fluid behaves like a Newtonian fluid with constant non-dimensional viscosity, $D = \mu_R$, in the region adjacent to the pipe wall. Thus, the value of D_w is μ_R for the modified power law model when A is large. Equation (79) indicates that $\gamma_w = \dfrac{2}{\mu_R}$ in the high shear rate regime characterized by $D_w = \mu_R$. In this flow regime, the non-dimensional wall shear-rate magnitude is over-predicted by the power law model.

4.4 The fully developed velocity distribution

The distributions of the axial velocity, w, are plotted in Figure 5 for various values of A. The velocity distribution in the *low shear rate regime*, predicted by the modified power law model, is displayed in Fig. 5(a). The velocity distribution predicted by the power law model when $A = 0.05$, is also shown in Fig. 5(a), for comparison. Typical velocity profiles in the *intermediate range of shear rate*s are shown in Figs. 5(b)-(d). The nature of the velocity distributions for values of A in the *high shear-rate* regime have been indicated in Figs. 5(e) and 5(f).

Fig. 5(a) shows that for $A = 0.05$, the velocity distribution predicted by the modified power law model is identical to the Hagen-Poiseuille velocity distribution for fully developed flow of a Newtonian fluid, given by equation (64). This is a consequence of the fact that in the low shear rate regime, the non-Newtonian viscosity predicted by the modified power law model is $D = 1$, everywhere in the flow field, as indicated by Fig. 3(a). All velocity distributions predicted using the modified power law model in the low shear rate regime are identical to the Hagen-Poiseuille velocity distribution (64). Thus, the Newtonian behavior of the non-Newtonian fluid at low shear rates is correctly reproduced by the modified power law model. Fig. 5(a) shows that the velocity profile predicted using the power law model is completely erroneous. The magnitudes of the velocity predicted using the power law model for $A = 0.05$ are much smaller than the magnitudes of the velocity for the Newtonian case. This is due to the fact that the non-Newtonian viscosities

predicted by the power law model are much higher than the zero shear-rate viscosity. Thus, the effective resistance of the hydraulic circuit is much higher in the case when the power law model is used, resulting in lower flow speeds.

Fig. 5(b) indicates that when A = 0.5, the velocity profile predicted by the power law model is closer to the velocity profile predicted by the modified power law model than for the case when A = 0.05. The velocity distribution predicted by the modified power law model for A = 0.5 differs slightly from the Hagen-Poiseuille velocity distribution. This may be explained with reference to Fig. 3(b) which shows that while D = 1 in the central region of the pipe, the viscosity distribution in the outer region of the pipe is governed by the power law.

Figs. 5(c) and 5(d) show that as the value of A is increased in the intermediate shear rate regime, the agreement between the velocity profiles predicted by the two models become closer. Fig. 5(c) indicates that when A = 1, the velocity distributions predicted by the modified power law and power law models are almost identical in the outer region near the pipe wall; the velocity distributions differ in a small region close to the axis of the pipe, where the velocity predicted using the power law model is slightly lower than the velocity predicted by the modified power law model, due to the larger viscosity. Fig. 5(d) shows that when A = 5, the velocity profiles predicted by the two models are identical on the scale of the graph.

Fig. 5(e) shows that velocity profiles predicted by the modified power law model and the power law model for A = 50 are also coincident, on the scale of the graph. This may be explained by referring to Fig. 3(e), which shows that the distributions of apparent viscosity predicted by the two models are identical except for a small region adjacent to the pipe wall where the viscosities differ slightly. The small difference in the effective resistance of the hydraulic circuit caused by this slight difference in the viscosities over a small region of the pipe does not lead to a significant difference in the flow speeds.

Figure 5(f) shows that the velocities predicted by the power law model when A = 750 are larger than the velocities predicted by the modified power law model. This may be explained with reference to Fig. 3(f) which shows that in the outer region adjacent to the pipe wall the apparent viscosities predicted by the power law model are lower than the constant viscosity, $D = \mu_R$, predicted using the modified power law. Thus, the effective resistance of the hydraulic circuit is lower in the case of the power law model, resulting in higher flow speeds.

4.5 Variation of the non-dimensional average velocity with *A*

The non-dimensional average velocity through the pipe, defined as the non-dimensional volume flow rate per unit cross-sectional area of the pipe, was determined using

$$w_{av} = \frac{1}{\pi} \int_0^1 2\pi\, r\, w(r)\, d\, r\,. \qquad (80)$$

The non-dimensional average velocity, $\left(w_{av}\right)_{PL}$, predicted using the power law model, is given by

$$\left(w_{av}\right)_{PL} = \frac{n+1}{3n+1} \left(\frac{2}{A^{n-1}}\right)^{\frac{1}{n}}. \qquad (81)$$

The non-dimensional average velocity, $\left(w_{av}\right)_{MPL}$, predicted by the modified power law model, was obtained by numerical integration.

The non-dimensional average velocity, $\left(w_{av}\right)_{MPL}$, predicted by the modified power law model, and the non-dimensional average velocity, $\left(w_{av}\right)_{PL}$, predicted using the power law model, have been tabulated in Table 1 for several values of *A*. The table shows that the average velocity predicted the power law model is lower than the average velocity predicted by the modified power law when the value of *A* is small. This is due to the fact that the apparent viscosities predicted by the power law model are higher than the apparent viscosities predicted by the modified power law model in the low shear rate regime, as indicated by Figs. 3(a) and (b). Thus, the effective resistance of the hydraulic circuit predicted by the power law model is higher than the effective resistance predicted by the modified power law model, resulting in lower flow speeds. It is worth noting that the average velocity predicted by the modified power law model for $A = 0.05$ is the same as the average velocity for a Newtonian fluid.

For $A = 5$ and $A = 50$, the average velocities predicted by the two models are almost identical. This may be explained by referring to Figs. 5(d) and 5(e). These figures show that the velocity profiles predicted by the two models for $A = 5$ and $A = 50$ are almost identical. Thus, in the *intermediate shear rate regime*, the agreement between the average velocities predicted by the power law model and the modified power law model is close.

At large values of *A*, the average velocity predicted by the power law model is higher than the average velocity predicted by the modified power law model. This may be explained using the

fact that in the *high shear rate regime* the apparent viscosities predicted by the power law model are lower than the apparent viscosities predicted by the modified power law model in the outer region adjacent to the pipe wall, as indicated by Figs. 3(e)and (f). Thus, the effective resistance of the hydraulic circuit predicted by the power law model is lower than the effective resistance predicted by the modified power law model, resulting in higher flow speeds.

4.6 The thermally developed temperature field

The radial distributions of the non-dimensional temperature, θ, are plotted in Fig. 6(a)-(f), for A = 0.05, 0.5, 1, 5, 50 and 750 respectively. The temperature profiles depicted in Fig. 6(a) are typical temperature profiles in the low shear rate regime, predicted by the modified power law model and the power law model. Typical temperature profiles in the *intermediate range of shear rate*s are shown in Figs. 6(b)-(d). The nature of the temperature distributions in the *high shear-rate* regime have been indicated in Figs. 6(e) and 5(f).

The temperature distribution predicted by the modified power law model when A = 0.05, shown in Fig. 6(a), is identical to the temperature distribution for thermally developed flow of a Newtonian fluid in a uniformly heated tube, given by equation (65). This is a consequence of the fact that in the low shear rate regime, the non-Newtonian viscosity predicted by the modified power law model is D = 1, everywhere in the flow field, as indicated by Fig. 3(a). The Newtonian behavior of the non-Newtonian fluid at low shear rates is correctly reproduced by the modified power law model. It is worth noting that all temperature distributions predicted using the modified power law model in the low shear rate regime are identical to the temperature distribution (65).

Fig. 6(a) shows that the prediction of the temperature distribution by the power law model is completely erroneous. The magnitudes of the temperature predicted using the power law model for A = 0.05, shown in Fig. 6(a), are much smaller than the magnitudes of the temperature for the Newtonian case. This may be explained with reference to equation (52). Equation (52) indicates that the non-dimensional temperature, θ, in the thermally developed region of the flow is obtained by solving a radial heat conduction equation with a source term, $w(r)$, which represents the effect of axial convection. Thus, the magnitudes of the temperature depend on the magnitudes of the velocity, $w(r)$. The magnitudes of the velocity predicted by the power law model for A =

0.05 are much smaller than the corresponding magnitudes of the velocity for a Newtonian fluid, as indicated by Fig. 5(a). Thus, the source term in the radial heat conduction equation (52) is under-predicted by the power law model, resulting in predictions of lower temperature.

Figs. 6(b)-(d) show that as the value of A is increased in an intermediate range of shear-rates, the agreement between the temperature profiles predicted by the two models become closer. This is because the velocity profiles predicted by the two models move closer with increase in the value of A, as indicated by Figs. 5(b)-(d). Consequently, the difference in the predictions of the source term in equation (52) by the two models decreases, leading to better agreement in the predicted temperatures.

A glance at Fig. 6(c) reveals that, when $A = 1$, the temperature profiles predicted by the two models are almost identical in the outer region of the pipe, and differ slightly in in a small region close to the axis of the pipe where the temperatures predicted by the power law model are slightly lower than the temperatures predicted by the modified power law model, as the corresponding velocity distributions, shown in Figure 5(c), differ slightly in the core region of the pipe. Fig. 6(d) shows that when $A = 5$, the temperature profiles predicted by the two models are identical on the scale of the graph.

Fig. 6(e) shows that temperature profiles predicted by the modified power law model and the power law model for $A = 50$ are also coincident, on the scale of the graph. This is due to the fact that the velocity profiles predicted by the two models are almost identical, as indicated by Fig. 5(e). Thus, the source term in the radial heat conduction equation (52) predicted by the two models are almost identical, leading to almost identical predictions of the temperature distribution.

Figure 6(f) indicates that when $A = 750$, the temperatures predicted by the power law model are much higher than the temperatures predicted by the modified power law model. This is because the velocities predicted by the power law model when $A = 750$ are larger than the velocities predicted by the modified power law model, as indicated by Figure 5(f). Consequently, the source term in the radial heat conduction equation (52) predicted by the power law model is much larger in magnitude compared to the source term predicted by the modified power law model, leading to predictions of higher temperatures.

4.7 Variation of the Nusselt number with *A*

Following [19, 20], the Nusselt number, defined as

$$Nu = \frac{q_w a}{k\left(T_w - T_0\right)}, \tag{82}$$

has been determined using the expression,

$$Nu\left(\frac{z}{Pe}\right) = -\left.\frac{d\theta}{dr}\right|_{r=1}. \tag{83}$$

The relation (83) follows from equations (14), (17), (18), (48) and (82). For a power-law fluid, the Nusselt number, Nu_{PL}, defined by equation (82), is given by

$$Nu_{PL}\left(\frac{z}{Pe}\right) = \frac{n}{2\left(3n+1\right)}\left(\frac{2}{A^{n-1}}\right)^{\frac{1}{n}}. \tag{84}$$

The relation (84) is easily derived from the temperature distribution for a power-law fluid, given in equation (62). The Nusselt number, Nu_{Newt}, for a Newtonian fluid, defined by equation (82), reduces to

$$Nu_{Newt}\left(\frac{z}{Pe}\right) = \frac{1}{4}, \tag{85}$$

[20]. The relation (85) is obtained from equation (84) by setting n = 1. The Nusselt number, Nu_{MPL}, predicted by the modified power law was determined from equation (83) using a three-point backward difference approximation.

The variation of $Nu(z/Pe)$ with A is plotted in Fig. 7, using logarithmic axes. The three regimes of flow are clearly seen in the prediction of the modified power law model. The solid line in Fig. 7, which represents the prediction of the modified power law model, shows that the value of $Nu(z/Pe)$ is independent of A when A is small. A glance at Fig. 7 reveals that the value of $Nu(z/Pe)$ predicted by the modified power law increases linearly with A on a logarithmic scale in the *intermediate shear rate regime*, and then appears to saturate in the *high shear rate regime*. As indicated by equation (84), the variation of $Nu(z/Pe)$ with A on a log-log plot is linear, for the power law model. This is indicated in Fig. 7 by the dashed line.

The constant value of $Nu(z/Pe)$ in the low shear-rate regime, predicted by the modified power law model, is equal to ¼ , the value of $Nu(z/Pe)$ indicated by equation (85) for a Newtonian fluid. This is a consequence of the fact that the non-Newtonian fluid behaves like a Newtonian fluid with constant non-dimensional viscosity, $D = 1$, in the low shear rate regime in the entire flow field. This Newtonian behavior of the fluid is correctly represented by the modified power law model, unlike the power law model which under-predicts the Nusselt number. The difference between the values of $Nu(z/Pe)$ predicted by the two models in the intermediate shear rate regime are too small to be seen on the scale of Fig. 7. In the high shear rate regime, the value of $Nu(z/Pe)$ predicted by the modified power law model asymptotically approaches a constant value.

5. Concluding remarks

The velocity and temperature distributions in hydrodynamically and thermally developed flow of a pseudoplastic fluid through a uniformly heated circular tube have been computed using a modified power law model. The parameters of the modified power law have been determined to fit available experimental data for the variation of the non-Newtonian viscosity of a 0.4 % polyacrylamide solution with shear-rate. The results predicted using the modified power law model with the rheological parameters chosen to fit existing experimental data have been compared with the results predicted by the power law model using the *same power law index*.

A non-dimensional *shear-rate parameter* governing the flow has been identified; this non-dimensional parameter, A, depends on the applied pressure gradient. The results indicate the existence of three distinct regimes of flow. These regimes have been classified as the low, intermediate and high shear-rate regimes. As the names suggest, the *low shear-rate regime* is characterized by small values of the shear rate parameter, A, and the *high shear-rate regime* is characterized by large values of A; the *intermediate shear rate regime* is characterized by values of A that are neither too small nor too large.

The modified power law model correctly predicts that the non-Newtonian fluid behaves as a Newtonian fluid in the low shear rate regime, with viscosity equal to the value of the zero-shear-rate viscosity. Consequently, the velocity and temperature distributions, and hence also the Nusselt number predicted by the modified power law are the same as that for a Newtonian fluid. In this low shear-rate regime, the power law model yields physically unrealistic predictions of

apparent viscosities higher than the zero-shear-rate viscosity everywhere in the flow field. In particular, the power law predicts that the apparent viscosity at the axis of the pipe is infinite. The velocity and temperature fields predicted by the power law are completely erroneous when the shear-rate parameter lies in the low shear rate regime. Due to the prediction of higher apparent viscosities, the magnitudes of the velocity and temperature predicted by the power law model are lower than the magnitudes of the velocity and temperature predicted by the modified power law model. Thus, the average velocity and Nusselt number predicted by the power law model in this regime are lower than that of a Newtonian fluid.

In the intermediate shear rate regime, the modified power-law predicts the existence of two distinct regions of flow: a central Newtonian region near the axis of the pipe where the apparent viscosity has a value equal to the zero-shear-rate viscosity and an outer power-law region adjacent to the pipe wall where the apparent viscosities follow the power law. The apparent viscosities predicted by the power law model in this outer region of flow agree with the apparent viscosities predicted by the modified power law model. In the central region, the power law model over-predicts the apparent viscosities, as in the case of the low shear rate regime. The velocity and temperature distributions predicted by the two models agree in the outer region of the pipe and differ in the central region where the values predicted by the power law model are lower, due to the increased viscosity. The relative sizes of the two regions depend on the value of the shear-rate parameter. As the value of A is increased, the central Newtonian region shrinks towards the axis of the pipe and the outer power law region adjacent to the pipe wall increases in size. Consequently, the agreement between the velocity and temperature distributions predicted by the two models becomes better as the value of A is increased in the intermediate range of shear rates. The Nusselt number predicted by the power-law agrees well with the Nusselt number predicted by the more realistic modified power model, in this intermediate shear rate regime.

In the high shear rate regime, the modified power law model predicts the existence of three distinct regions of flow: a central Newtonian region near the axis of the pipe where the apparent viscosity is equal to the zero-shear-rate viscosity, an outer Newtonian region adjacent to the pipe wall where the apparent viscosities is equal to the infinite-shear-rate viscosity, and a middle power-law region between these two distinct Newtonian regions where the apparent viscosities follow the power law. In the outer region, the power law model yields physically unrealistic predictions of apparent viscosities lower than the infinite-shear-rate viscosity. The apparent

viscosities predicted by the power law model agree with the apparent viscosities predicted by the modified power law model in the middle region of flow. In the central region, the power law model yields physically unrealistic predictions of apparent viscosities higher than the zero-shear-rate viscosity. However, the size of the central region is very small as A is large; hence, this region does not significantly influence the values of global quantities such as the average velocity and Nusselt number. Due to the prediction of lower apparent viscosities in the outer region, the magnitudes of the velocity and temperature predicted by the power law model are higher than the magnitudes of the velocity and temperature predicted by the modified power law model. Consequently, the average velocity and Nusselt number predicted by the power law model in this regime are higher than that of a Newtonian fluid.

The importance of the shear-rate parameter, A, has been clearly demonstrated by the results presented in the paper. It has been shown that the power law model yields physically unrealistic predictions when A is small or large. The effects of the new parameter A on non-Newtonian viscosity and consequently on the fluid flow are clearly demonstrated in [29].

Figures and Tables

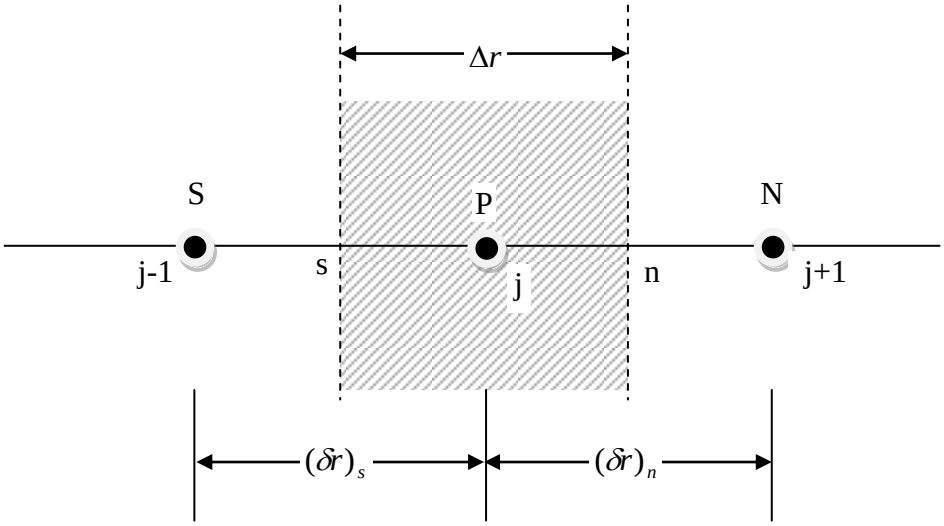

Fig. 1: A regular control volume

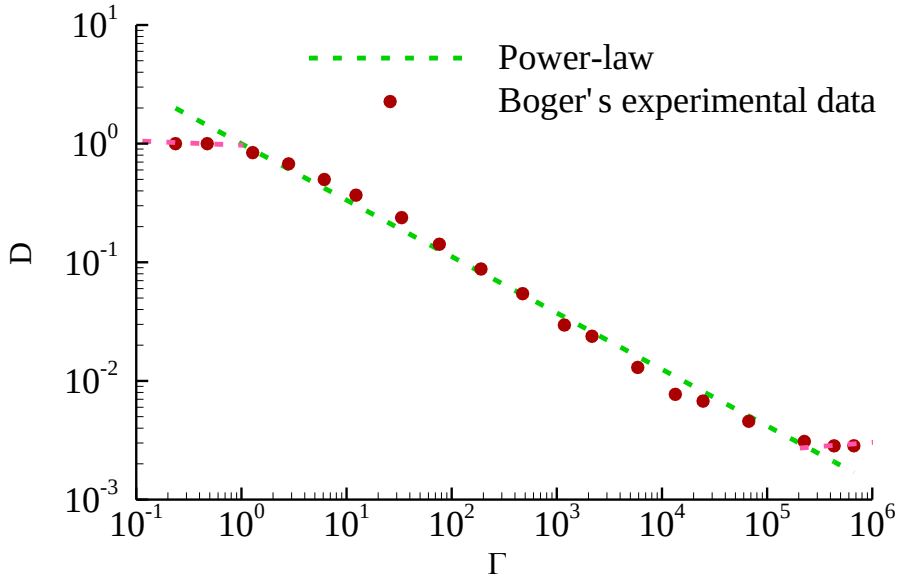

Fig.2: Variation of the non-dimensional viscosity, $D = \mu / \mu_0$, with the magnitude of the non-dimensional shear rate, Γ. The circles represent experimental data from Boger [15]. The reference viscosity is μ_0 =1.42 kgm^{-1}s^{-1}.

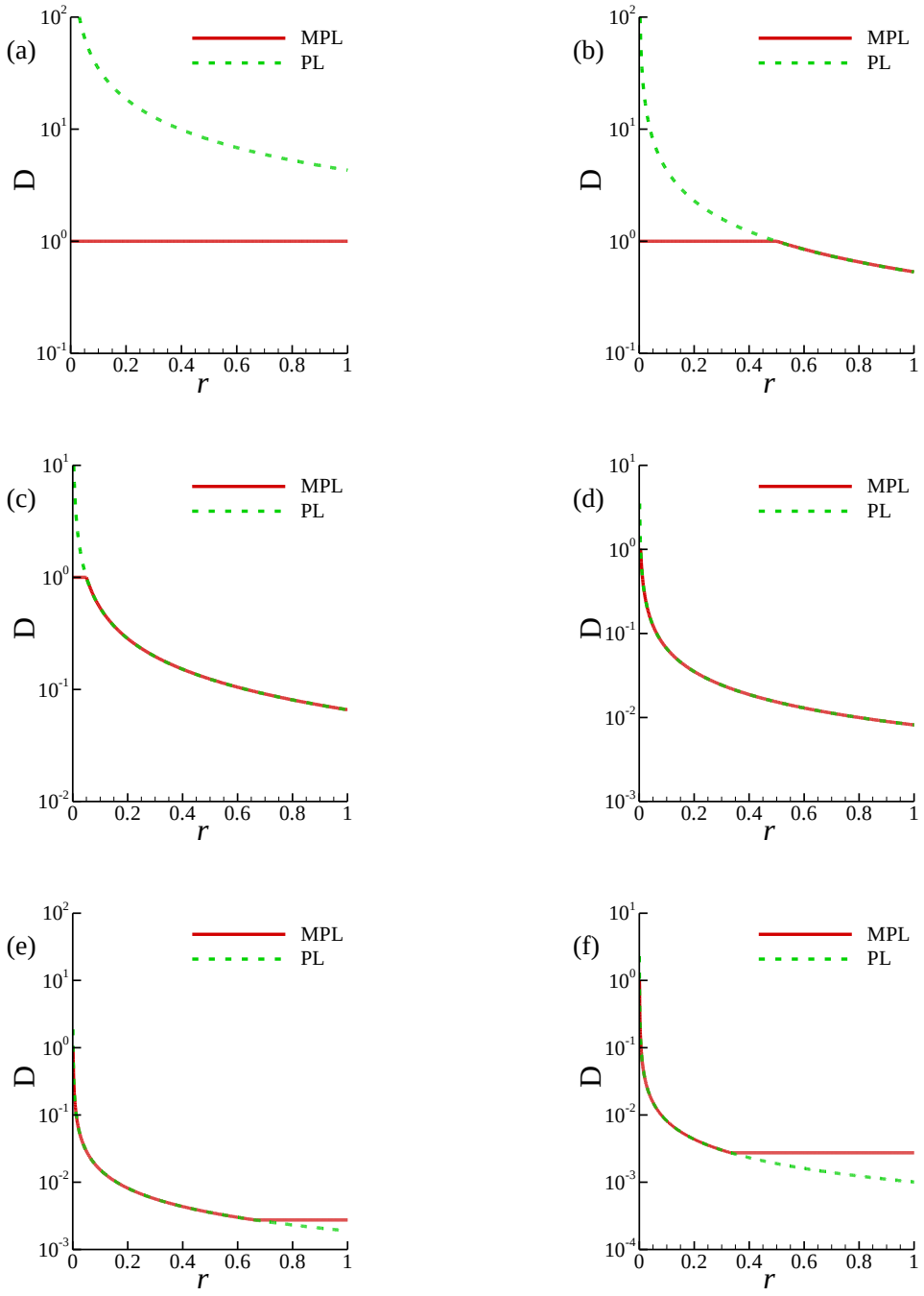

Fig. 3: Radial distribution of non-Newtonian viscosity for (a) A = 0.05, (b) A = 0.5, (c) A = 1, (d) A = 5, (e) A = 50 and (f) A = 750.

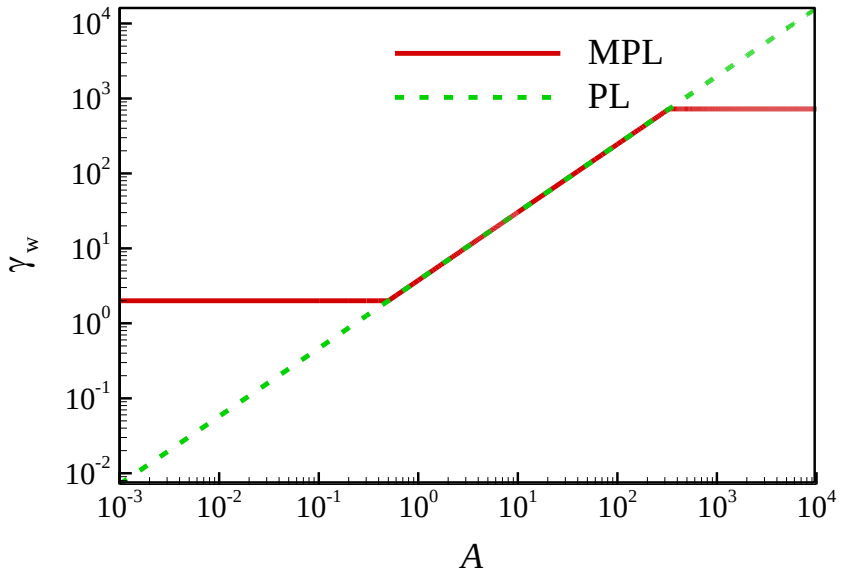

Fig. 4: **Variation of the non-dimensional wall shear-rate magnitude, γ_w , with *A*.**

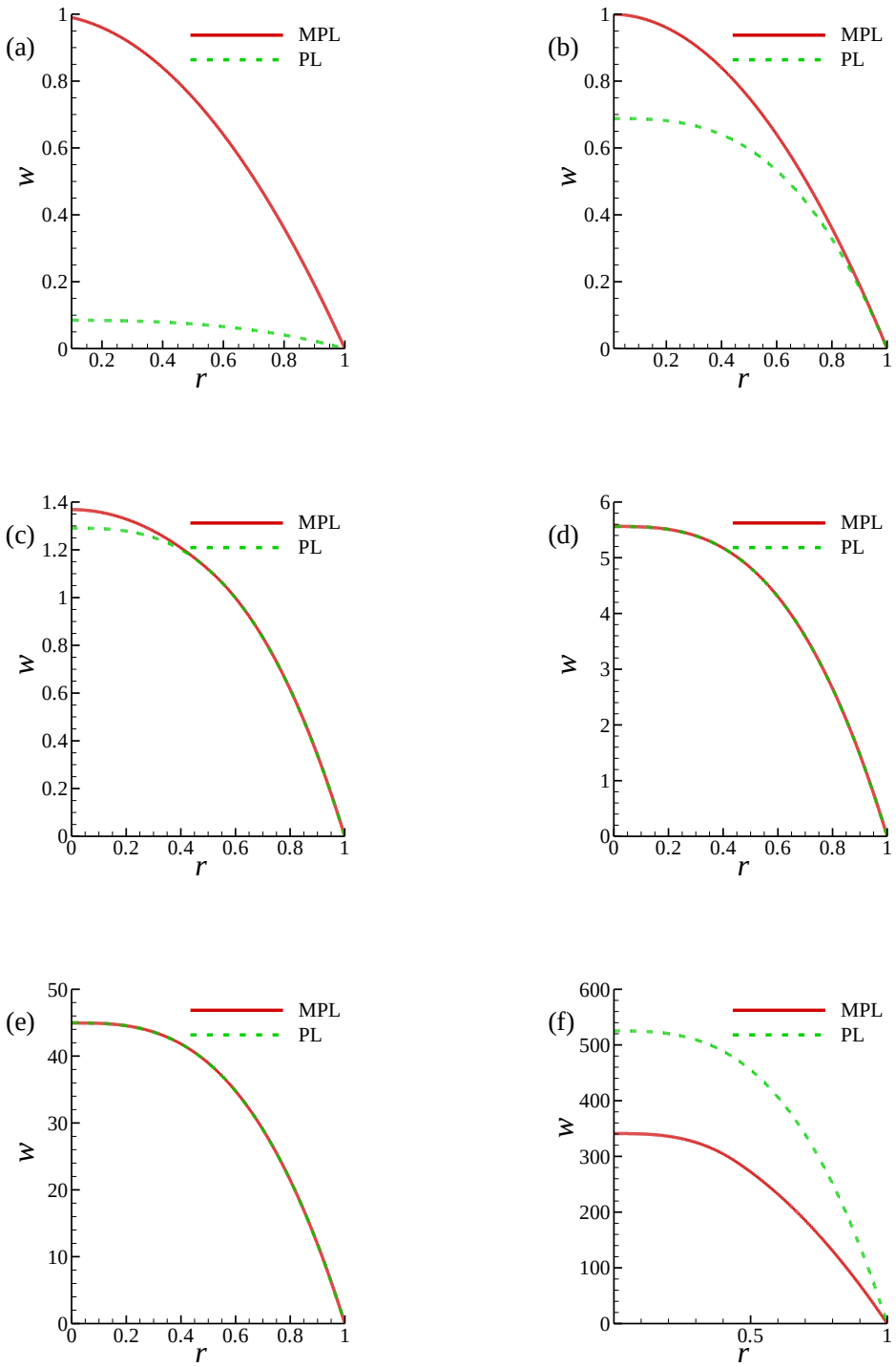

Fig. 5: Axial velocity distribution for (a) A = 0.05, (b) A = 0.5, (c) A = 1, (d) A = 5, (e) A = 50 and (f) A = 750.

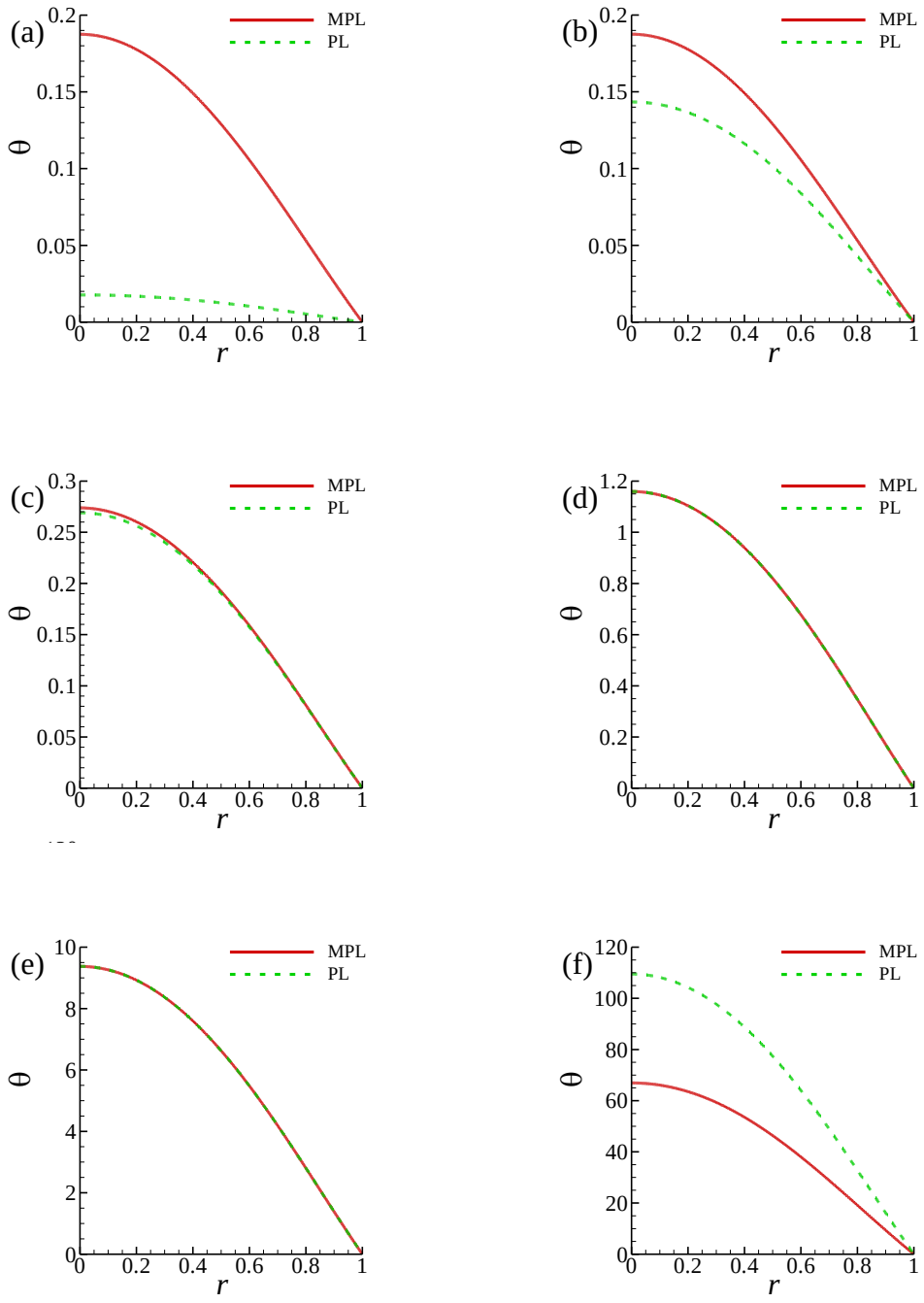

Fig. 6: Temperature distribution for (a) A = 0.05, (b) A = 0.5, (c) A = 1, (d) A = 5, (e) A = 50 and (f) A = 750.

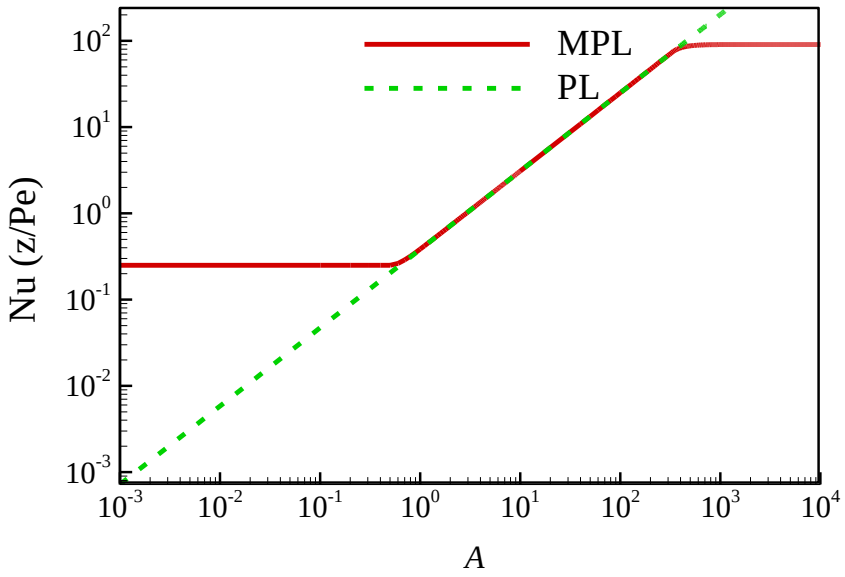

Fig.7: Variation of the Nusselt number with *A*.

Table 1. Variation of the non-dimensional average velocities predicted by the power law model and the modified power law model with *A*

A	$(w_{av})_{PL}$	$(w_{av})_{MPL}$
0.05	0.05041	0.5
1	0.7645	0.7703
5	3.29476	3.29477
50	26.63743	26.63743
750	311.16717	180.23208
1000	404.01433	181.09822

References

[1] Yao, L.S., and Molla, M.M., "Non-Newtonian Fluid Flow on a Flat Plate Part I: Boundary Layer," *Journal of Thermophysics and Heat Transfer*, Vol. 22, 2008, pp. 758-761.

[2] Molla, M.M., and Yao, L.S, "Non-Newtonian Fluid Flow on a Flat Plate Part II: Heat Transfer," *Journal of Thermophysics and Heat Transfer*, Vol. 22, 2008, pp. 762-765.

[3] Yao, L.S., and Molla, M.M., "Forced Convection of Non-Newtonian Fluids on a Heated Flat Plate," *International Journal of Heat and Mass Transfer*, Vol. 51, 2008, pp. 5154-5159.

[4] Molla, M.M., and Yao, L.S., "The Flow of Non-Newtonian Fluid on a Flat Plate with a Uniform Heat Flux," *Journal of Heat Transfer*, Vol. 131, 2009, pp. 011702-1~6.

[5] Molla, M.M., and Yao, L.S., "Non-Newtonian Natural Convection Along a Vertical Heated Wavy Surface using a Modified Power-law Viscosity Model," *Journal of Heat Transfer*, Vol. 131, 2009, pp. 012501-1~6.

[6] Molla, M.M., and Yao, L.S., "Non-Newtonian Natural Convection Along a Vertical Plate Heated with Uniform Surface Heat Fluxes," *Journal of Thermophysics and Heat Transfer*, Vol. 23, 2009, pp. 176-185.

[7] Molla, M.M., and Yao, L.S., "Mixed Convection of Non-Newtonian Fluids Along a Heated Vertical Flat Plate," *International Journal of Heat and Mass Transfer*, Vol. 52, 2009, pp. 3266-3271.

[8] Ghosh Moulic, S., and Yao, L.S., "Non-Newtonian Natural Convection Along a Vertical Flat Plate with Uniform Surface Temperature," *Journal of Heat Transfer*, Vol. 131, 2009, pp. 062501-1~8.

[9] Bhowmick, S., Molla, M.M. and Yao, L.S., "Non-Newtonian Mixed Convection Flow along a Horizontal Circular Cylinder," *Numerical Heat Transfer, Part A: Applications: An International Journal of Computation and Methodology*, Vol. 66(5), 2014, pp. 509-529.

[10] Hinch, J., "Non-Newtonian Geophysical Fluid Dynamics," *Conceptual Models of the Climate*:*2003 Program in Geophysical Fluid Dynamics*, Woods Hole Oceanographic Institution, Woods Hole, MA, 2003.

[11] Bird, R.B., Armstrong, R.C., and Hassager, O., *Dynamics of Polymeric Liquids, Vol. 1, Fluid Mechanics*, 2nd ed., Wiley, New York, 1987.

[12] Chhabra, R.P., and Richardson, J.F., *Non-Newtonian Flow in the Process Industries, Fundamentals and Engineering Applications*, Butterworth Heinemann, Oxford, 1999.

[13] Chhabra, R.P., and Richardson, J.F., *Non-Newtonian Flow and Applied Rheology: Engineering Applications*, 2nd ed., Butterworth Heinemann, Oxford, 2008.

[14] Bird, R.B., Stewart, W.E., and Lightfoot, E.N., *Transport Phenomena*, 2nd ed., Wiley, New York, 2002.

[15] Boger, D.V., "Demonstration of Upper and Lower Newtonian Fluid Behaviour in a Pseudoplastic Fluid," *Nature*, Vol. 265, 1977, pp. 126-128.

[16] Bejan, A., *Entropy Generation Minimization: The Method of Thermodynamic Optimization of Finite-Size Systems and Finite-Time Processes*, CRC Press, Boca Raton, 1996.

[17] Naterer, G.F. and Camberos, J.A., *Entropy-Based Design and Analysis of Fluids Engineering Systems*, CRC Press, Boca Raton 2008.

[18] Bejan, A., *Convection Heat Transfer*, 3rd ed., Wiley, New Jersey, 2004.

[19] Morton, B.R., "Laminar convection in uniformly heated horizontal pipes at low Rayleigh numbers," *The Quarterly Journal of Mechanics and Applied Mathematics*, Vol. 12, 1959, pp. 410-420.

[20] Yao, L.S. and Berger, S.A., "Flow in heated curved pipes," *Journal of Fluid Mechanics*, Vol. 88, 1978, pp. 339-354.

[21] Prusa, J. and Yao, L.S., "Numerical solution for fully developed flow in heated curved tubes," *Journal of Fluid Mechanics*, Vol. 123, 1983,pp. 503-522.

[22] Yao, L.S. and Ghosh Moulic, S., "Uncertainty of convection," *International Journal of Heat and Mass Transfer*, Vol. 37, 1994, pp. 1713-1721.

[23] Yao, L.S. and Ghosh Moulic, S., "Nonlinear instability of travelling waves with a continuous spectrum," *International Journal of Heat and Mass Transfer*, Vol. 38, 1995, pp. 1751-1772.

[24] Yao, L.S., "Is a fully developed and non-isothermal flow possible in a vertical pipe?," *International Journal of Heat and Mass Transfer*, Vol. 30, 1987, pp. 707-716.

[25] Yao, L.S., "Linear stability analysis for opposing mixed convection in a vertical pipe," *International Journal of Heat and Mass Transfer*, Vol. 30, 1987, pp. 810-811.

[26] Rogers, B.B. and Yao, L.S., "Finite amplitude instability of mixed convection in a heated vertical pipe," *International Journal of Heat and Mass Transfer*, Vol. 36, 1993, pp. 2305-2315.

[27] Rogers, B.B. and Yao, L.S., "The effect of mixed convection instability on heat transfer in a vertical annulus," *International Journal of Heat and Mass Transfer*, 1990, Vol. 33, 1990, pp. 79-90.

[28] Rogers, B.B. and Yao, L.S., "Finite amplitude instability of mixed convection in a heated vertical annulus," *Proceedings of the Royal Society of London Series A*, Vol. 437, 1992, pp. 267-290.

[29] Yao, L.S., Molla, M.M. and, Ghosh Moulic, S., "Fully-Developed Circular-Pipe Flow of a Non-Newtonian Pseudoplastic Fluid," *Universal Journal of Mechanical Engineering*, Vol. 1(2), 2013, pp. 23-31.

[30] Patankar, S.V., *Numerical Heat Transfer and Fluid Flow*, Hemisphere Publishing Corporation, Washington, 1980.

[31] Neofytou, P., A third order upwind finite volume method for generalized Newtonian fluid flows, *Adv. Eng. Softw*. Vol.36 (2005) pp.664-680

[32] Bell, B. C. and Surana, K. S., P verersion least squares finite elements formulation for two-dimensional, incompressible, non-Newtonian and isothermal flow, *Int. J. Numer. Methods Fluids*, Vol.18 (1994) pp 127-162.